EXPERIMENTAL INVESTIGATION OF BOUNDARY LAYER BEHAVIOR
IN A SIMULATED LOW PRESSURE TURBINE

Rickey J. Shyne
Senior Research Engineer
NASA Glenn Research Center
Cleveland, Ohio 44135

Ki-Hyeon Sohn
Research Associate
University of Toledo
Toledo, Ohio 43606

Kenneth J. De Witt
Professor
University of Toledo
Toledo, Ohio 43606

ABSTRACT

A detailed investigation of the flow physics occurring on the suction side of a simulated Low Pressure Turbine (LPT) blade was performed. A contoured upper wall was designed to simulate the pressure distribution of an actual LPT blade onto a flat plate. The experiments were carried out at Reynolds numbers of 100,000 and 250,000 with three levels of freestream turbulence. The main emphasis in this paper is placed on flow field surveys performed at a Reynolds number of 100,000 with levels of freestream turbulence ranging from 0.8% to 3%. Smoke-wire flow visualization data was used to confirm that the boundary layer was separated and formed a bubble. The transition process over the separated flow region is observed to be similar to a laminar free shear layer flow with the formation of a large coherent eddy structure. For each condition, the locations defining the separation bubble were determined by careful examination of pressure and mean velocity profile data. Transition onset location and length determined from intermittency profiles decrease as freestream turbulence levels increase. Additionally, the length and height of the laminar separation bubbles were observed to be inversely proportional to the levels of freestream turbulence.

NOMENCLATURE

C_P Static pressure coefficient $[=2(P-P_{exit})/\rho U^2_{exit})]$

E   Hot-film gage voltage, volts

H   Bubble height, cm

L   Effective working plate length, cm

$\bar{P}$ Gaster's pressure parameter $[= (\theta_s^2/v)(\Delta U/\Delta x)]$

Re   Test section Reynolds number $[=U_{exit}L/v]$

Re_{L_T} Transition length Reynolds number

Re_{θ_s} Momentum thickness Reynolds number at separation $[=U_s\theta_s/v]$

Tu   Local freestream turbulence level

U   Axial mean velocity, m/sec

u'_{rms} Axial fluctuating velocity, m/sec

X, x   Axial distance from leading edge, cm

y   Normal distance from surface, cm

Greek

δ Boundary layer thickness at $U/U_e=0.995$, cm

δ^* Displacement thickness $\left[= \int_0^y (1 - u/u_e)dy\right]$, cm

θ Momentum thickness $\left[= \int_0^y u/u_e (1 - u/u_e)dy\right]$, cm

Γ Intermittency

Λ Longitudinal integral length scale, cm

ψ_i Stream function $\left[= \int_0^{y_i} (U / U_{ref}) dy\right]$

v Kinematic viscosity, m^2/sec

Subscripts

B   Bubble

e   Edge of boundary layer

R   Reattachment

ref   Reference

S   Separation

T   Transition

ex   Exit

INTRODUCTION

Gas turbine engine designers are constantly seeking ways to improve engine efficiency. The engine performance at cruise conditions, especially the behavior of engine components such as the low pressure turbine (LPT), is less clear due to limitations of ground test facilities to model altitude flight conditions. Many factors are known to influence the performance of the LPT, but factors such as blade loading, end wall losses, wake passing effects and boundary layer separation and/or transition play a major role. The accurate prediction of the separation and transition processes on LPT blades under the influence of adverse pressure gradients, altitude Reynolds

numbers and various freestream turbulence levels can lead directly to improved engine efficiency and lower specific fuel consumption. The primary objective of this experimental study is to determine whether the boundary layer flow on the suction side of a simulated LPT blade undergoes separation under cruise type flight conditions independent of wake passing, curvature or endwall effects. Additionally, if separation does occur, it is desired to characterize the separation bubble. This characterization is required because the chordwise extent of a separation bubble at high freestream turbulence and low Reynolds number is not large enough to alter the global flow pattern. However, a significant problem exists in defining an initial boundary condition for calculating the turbulent boundary layer at the downstream end of the bubble.

Gardner (1981) performed experimental studies on the effect of loading on LPT blades. The results showed that when designed properly, highly loaded blades exhibit higher performance than blades designed with a lower loading profile. Because of this study and others, modern LPT blades are now designed to be more highly loaded with lower aspect ratios that introduce highly adverse as well as highly favorable pressure gradients into the flow field. Halstead et al. (1995) performed an experimental study of boundary layer development on the suction surface of airfoils in an embedded stage of a LPT. This study revealed substantial regions of laminar and transitional flow on the suction surface, but no flow separation was apparent. This study also showed that the calmed regions, generated by the turbulent spots produced in the wake paths, were effective in suppressing the flow separation. Morin & Patrick (1991) performed a detailed study of a large-scale laminar separation bubble on a flat plate. It was determined from this experiment that the reattachment location of a short bubble was time dependent. Since the boundary layer approaches steady state very slowly, conventional eddy-viscosity models for the turbulent boundary layer were not valid until far downstream from the reattachment location. A fully turbulent boundary layer was not achieved even after 200 bubble heights downstream from the reattachment location. It can be deduced from these experimental studies that a short separation bubble can play a critical role in defining the initial boundary condition for the turbulent boundary layer calculation.

The present experimental study was conducted on a simulated LPT blade test section. The differences in the transition processes between the separated and attached boundary layers were studied qualitatively and quantitatively. Flow visualization, pressure, mean and fluctuating velocities and instantaneous hot-film data are used to analyze the flow-field simulated in this experiment.

EXPERIMENTAL FACILITY

The experiments were performed in a low-speed, closed-loop wind tunnel located at the NASA Glenn Research Center. This wind tunnel was designed to generate large scale, two-dimensional, incompressible boundary layers. Freestream turbulence levels in the test section were changed by the use of turbulence generating grids. A detailed description of the tunnel components can be found in Suder et al. (1988).

A contoured upper wall was designed to generate a pressure distribution on the bottom flat test surface that matches the pressure gradient generated by the suction surface of a generic LPT blade. To properly match the Reynolds number in a full scale LPT, a splitter plate was inserted in the middle of the test section to bifurcate the test section flow. The schematic of the test section is shown in Fig. 1. The splitter plate, which also doubled as the test flat plate, has a 4:1 elliptical leading edge and a trailing deflector which forces the stagnation point to fall on top of the working surface at the leading edge by generating circulation. The test plate was instrumented with fourteen flush-mounted hot-film gages located at 1.27-cm intervals along the centerline and eighteen static pressure taps located 2.54-cm off of the plate centerline.

An engine company supplied the generic LPT blade geometry. The test section design was created by matching the mass flow from the generic LPT blade cascade through a flow channel with a contoured upper wall and a flat lower wall. An inviscid panel code developed by McFarland (1982) was used to compute the blade velocity and pressure distribution. The flow field data computed by the panel code are functions of the area change throughout the channel. One and two body options were used in the panel code to generate the upper wall and the continuity equation was utilized to account for the difference between the two options. Details of this procedure can be found in Shyne (1998).
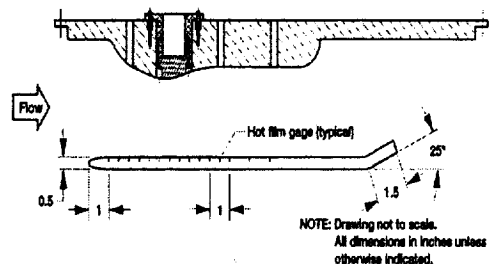

Figure 1. Schematic of simulated test section (1 in. =2.54 cm)

EXPERIMENTAL RESULTS

Detailed flow field measurements were obtained over the entire flat plate for both accelerating and decelerating flow regions at Reynolds numbers of 100,000 and 250,000 with various levels of freestream turbulence. The Reynolds number is based upon the effective working plate length of 15.50 cm and the exit freestream velocity. The primary emphasis of this paper is placed on flow field surveys in the adverse pressure gradient region at a Reynolds number of 100,000 with three nominal freestream turbulence levels of 0.8% (grid 0), 2% (grid 2) and 3% (grid 3). The profiles were obtained at ten measurement stations ranging from x=12.07 cm to x=23.50 cm from the leading edge of the flat plate in increments of 1.27 cm. Hot wire measurements in the spanwise direction showed no flow variation. The longitudinal integral length scales computed from power spectral density data are summarized in Table 1. The integral length scale increases as the turbulence level increases and this is consistent for both Reynolds numbers tested.

Flow Visualization

Smoke wire flow visualization was conducted to capture the qualitative features of the flow. This flow visualization was performed with grid 0 at a Reynolds number of 50,000 (based on an exit velocity of 4.92 m/s), which is lower than the typical cruise Reynolds number. Three instantaneous photographs of flow visualization are shown in Fig. 2 and show the presence of a laminar separation bubble. Due to rapid dispersion of the smoke at higher Reynolds numbers and intense mixing with higher turbulence levels, good quality photographs could

not be obtained for higher Reynolds numbers and higher turbulence conditions. No smoke is present in the region between the separated shear layer and the test surface within the front part of the separation bubble due to infinitesimal viscous shear stresses. The flow fields in this so-called 'dead-air' region look similar in each photograph, which indicates that the laminar region of the separation bubble is steady. However, a difference in the flow pattern in the region downstream of the maximum bubble height reveals that the transition and the reattachment processes are unsteady. A large eddy structure is apparent in the photographs downstream from the maximum bubble height in the shear layer. These eddies eventually become unstable and, through interaction with each other, finally develop into a turbulent boundary layer. This transition process is similar in behavior to a laminar free shear layer flow, where discrete spanwise vortices form due to the Kelvin-Helmholtz instability and eventually break down into a fully turbulent shear layer. A detailed flow visualization study performed by Morin and Patrick (1991) also revealed this eddy formation in the shear layer.
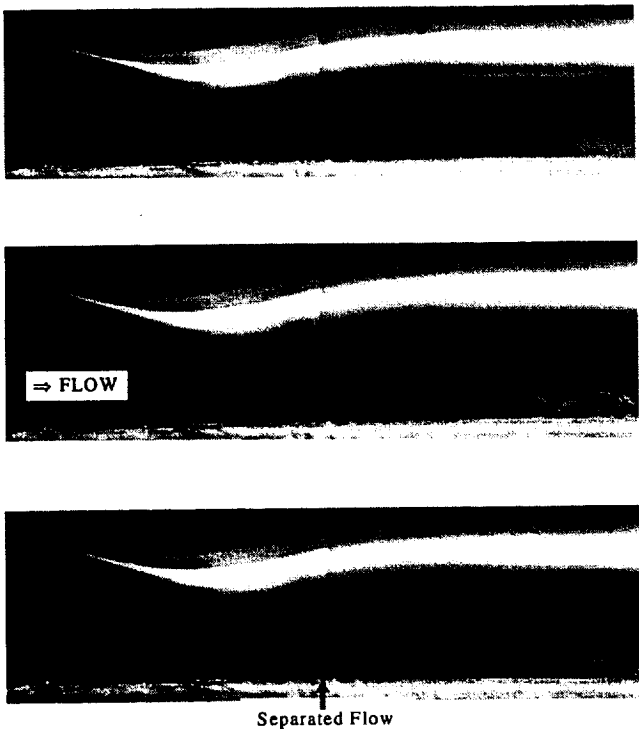

⇒ FLOW

Separated Flow

Figure 2. Smoke-wire flow visualization of separation bubble, Grid 0, Re = 50,000

Streamwise Pressure Distributions

Static pressure distributions were obtained on the surface of the flat plate at three levels of freestream turbulence. The variation of pressure coefficient, C_p, based on exit static and total pressures for a Reynolds number of 100,000 is presented in Fig. 3. The flow is accelerated up to the suction peak in the converging section and then is decelerated by the adverse pressure gradient. If the adverse pressure gradient is sufficient, the laminar boundary layer reaches separation before transition is achieved. As shown in Fig. 3, after the suction peak, the pressure increases steadily and then reaches a nearly constant level because of negligible turbulent diffusion in the laminar part of

the separated flow region. This constant pressure plateau is identified as the dead-air region in the flow visualization. Downstream from the constant pressure region the pressure rises sharply for a short distance to a certain point, then slowly increases to the exit pressure level. For each freestream turbulence level tested, the beginning of the constant pressure region is nearly identical (13.34 cm), within experimental error, indicating that the freestream turbulence level has little or no effect on the separation location. However, with increasing freestream turbulence level, the extent of the constant pressure region progressively shrinks and the downstream end of the sudden pressure rise (reattachment location) moves upstream, indicating the overall bubble length has decreased. These positions are summarized in Table 2 and are indicated by the arrows in Fig. 3 for grid 0.
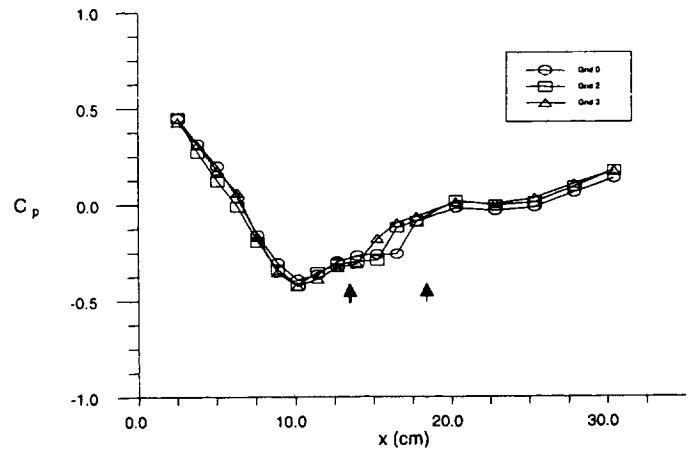

Figure 3. Pressure distribution on the test plate. (Re = 100,000), $\Delta C_p = \pm 0.005$

Hot-film Voltage Traces

A series of flush-mounted hot-film gages were used to identify the transition process. The typical instantaneous hot-film voltage traces for grid 2 and Reynolds numbers of 100,000 and 250,000 are shown in Figs. 4a-b. A typical stable laminar boundary layer signal can be seen in the first voltage trace at x=12.70 cm. A steady signal is obvious in the second voltage trace at x=13.97 cm in Fig. 4a because it is in the laminar portion of the separation bubble (refer to Table 2 for the streamwise location of bubble). An oscillating signal with high frequency components is shown in the third voltage trace and grows rapidly through the transition and reattachment region (x=15.24 and 17.78 cm). The signals at these locations become more random in character and finally develop into a fully turbulent signal.

Figure 4b shows the series of hot-film traces for a Reynolds number of 250,000. Due to the increased Reynolds number, the transition location moves upstream of the point where laminar separation would occur. Consequently, the increased wall shear stress resulting from the boundary layer transition keeps the boundary layer from separating at this Reynolds number. In Fig. 4b, intermittent turbulent spots can be clearly seen in the second trace at x=13.97 cm. These turbulent spots are formed more frequently as the flow proceeds downstream (from x=13.97 cm to x=17.78 cm). It can be seen from the hot-film traces in Fig. 4b that transition is initiated between x=12.70-13.97 cm, whereas the boundary layer separates for a Reynolds number of 100,000 (Fig. 4a). This transition process

3

follows the typical path for an attached boundary layer through the formation of turbulent spots.
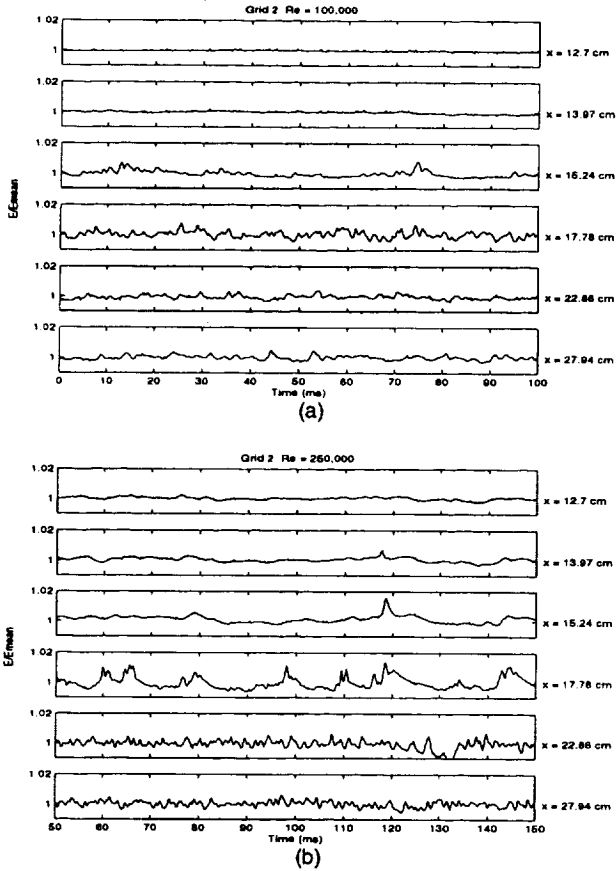
Figures 4a-b. Flush-mounted hot-film signals for Grid 2
(a) Re = 100,000 and (b) Re = 250,000, ΔE= ± 0.0004

Mean Velocity Profiles

To further investigate this complex flow field at a Reynolds number of 100,000, streamwise mean and fluctuating velocity profiles were measured with a single hot-wire probe. Figures 5a-c present the variation of the mean velocity profile normalized with the freestream velocity at the first measurement station under the adverse pressure gradient (x=12.07 cm) for each condition. The stream function, ψ_i, was determined by integrating the mean velocity at any point y_i up to the vicinity of the upper wall, which is

$$\psi_i = \int_0^{y_i} U/U_{ref}\,dy.$$

Equal values of ψ_i used to define the streamline patterns are also shown in Figs. 5a-c for each condition. The profile at the first measurement station has an inflection point imposed by the adverse pressure gradient (at x=12.07 cm), which is the precursor of boundary layer separation. A small hump in the streakline patterns downstream of the first measurement station was detected for each condition. Due to the inability of the hot-wire to determine the flow direction, no reverse flow could be detected. Instead, nearly constant velocity profiles were measured near the test surface in the separated flow region. The maximum bubble height was determined by interpolating the extent of this constant velocity region and is listed in Table 2 for

each condition. It can be noted that the bubble length and height are all inversely proportional to the freestream turbulence level. The uncertainty in the hot-wire measurements was determined to be 1.45%
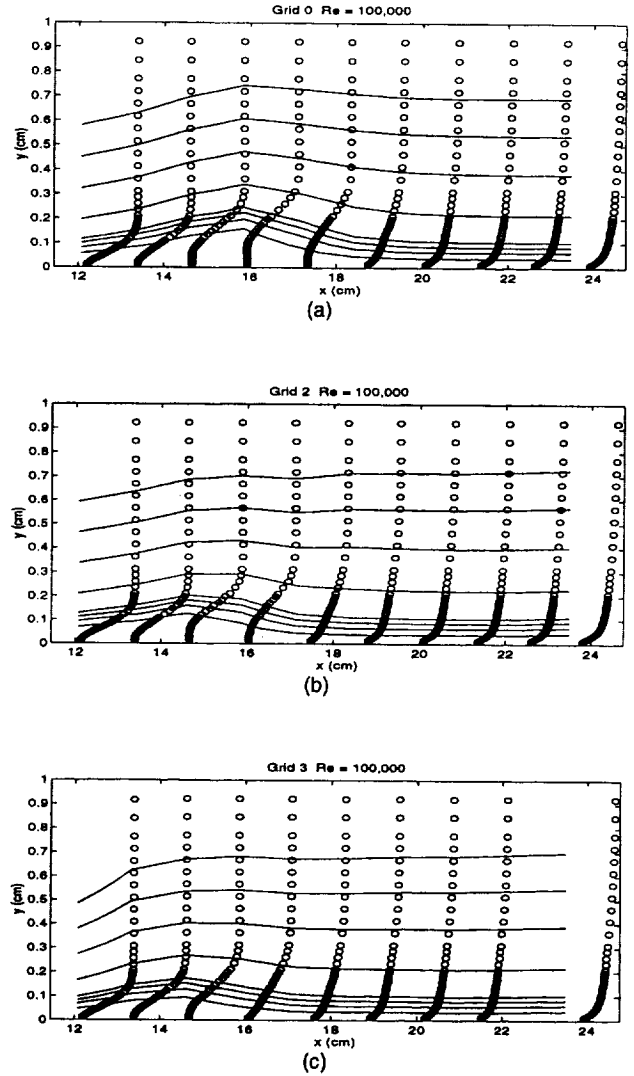
Figure 5a-c. Distribution of U/U_ref for Grids 0, 2 and 3
Re = 100,000 (U_ref=U_e at x=12.07 cm), ΔU= ± 0.00145

for the mean and fluctuating velocity components using methods developed by Yavuzkurt (1984). The error in the pressure and temperature measurements are ± 0.05 kPa and ± 0.3 °C, respectively.

The flow near the wall is distorted by the bubble. As shown in Fig. 5b, the velocity profile just downstream of the bubble (x=17.78 cm) shows double inflection points and finally develops into a fully attached turbulent boundary layer further downstream. Generally, these short bubbles only alter the local flow field, not affecting the global flow pattern away from the wall.

4

Intermittency Profiles

Intermittency profiles were also computed from the digitally recorded instantaneous velocity profile data and are shown in Figs. 6a-c. Intermittency, Γ, is defined as the fraction of time during which the flow at a given position remains turbulent after the onset of transition. A flow is considered fully turbulent if $\Gamma = 1$ and fully laminar if $\Gamma = 0$. The instantaneous velocity signal was segregated into turbulent and non-turbulent parts based on both of the squares of the first and second derivatives of the signals. The detailed technique can be found in Sohn & Reshotko (1991) and necessary integral boundary layer quantities are available in Shyne (1998). Figure 6a is an intermittency profile plot for grid 0 and it shows that transition begins between x=14.60 and x=15.87 cm. A peak intermittency value occurs for x=15.87 cm at an approximate y/δ value of 0.5.
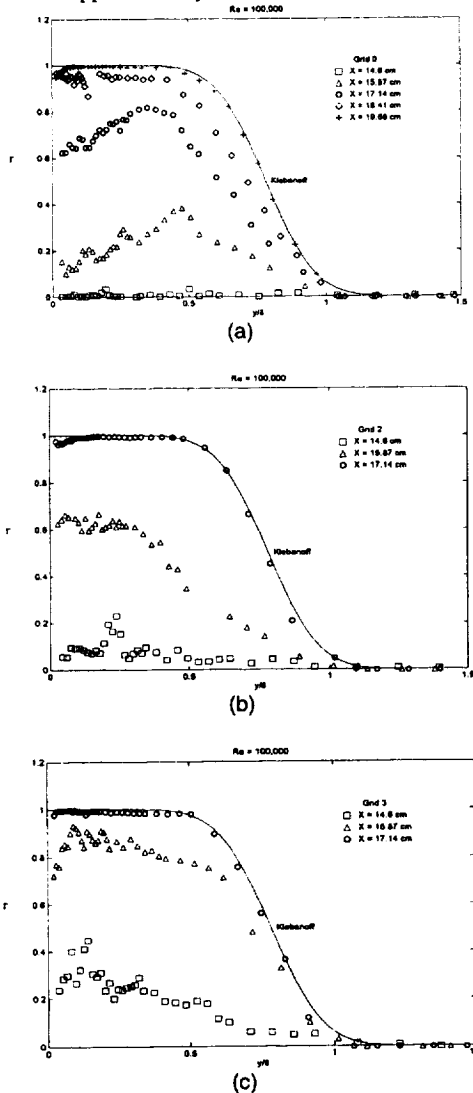

(a)

(b)

(c)

Figure 6a-c. Intermittency profiles, Re =100,000
(a) Grid 0 (δ=0.125 cm), (b) Grid 2 (δ=0.128 cm) and (c) Grid 3 (δ=0.129 cm), $\Delta\Gamma$= ± 1.45%

As the flow proceeds downstream in the test section, the peak intermittency values move towards the wall with the flow becoming fully turbulent. Figures 6b and c are the intermittency profile plots for grids 2 and 3. These plots exhibit similar trends to the grid 0 intermittency plot, but the transition point moves upstream and the transition length decreases. This transition process occurs in the shear layer, which bounds the freestream flow and bubble surface. Additionally, the flat portions of the intermittency profiles for y/δ values less than 0.2 for each condition correspond to the constant velocity region inside the separation bubble. Shear flow transition starts at approximately x=14.60 cm for grid 2 and before x=14.60 cm for grid 3, respectively. Peak intermittency values occur for grid 2 at x=14.60 cm at a y/δ value of approximately 0.25. Fully turbulent flow occurs at approximately x=17.14 cm for grid 2 and at approximately x=15.87 - 17.14 cm for grid 3. Approximate transition onset and fully turbulent flow locations obtained from the intermittency profiles agree favorably with those deduced from the hot-film data for each condition.

RMS Velocity Profiles

The fluctuating rms velocity profiles are shown in Fig. 7 for grid 0 along with the same streamline patterns plotted for the mean velocity profiles in Fig. 5a. Figures 8a-c show the normalized rms velocity profiles for grids 0, 2 and 3 and a Reynolds number of 100,000. In the laminar boundary layer at a low freestream turbulence level (grid 0), the rms velocity profile shows nearly a flat profile with small magnitudes for the entire flow field except for a small hump near the wall. This small first peak grows in magnitude and moves away from the wall to the shear layer as the flow goes downstream from the separation location. This peak in the shear layer grows rapidly after the maximum bubble height location and triggers a slowdown of bubble growth due to turbulent energy dispersion. For higher freestream turbulence levels (grids 2 and 3), the peak is much larger than that for grid 0 at the first measurement station because the laminar boundary layer is buffeted by higher freestream turbulence. Note that the fluctuating velocity profiles measured at the last measurement station (x=23.50 cm) are different from that of the equilibrium turbulent boundary layer measured by Klebanoff (1955) for each condition. This indicates that even though an attached turbulent boundary layer profile was measured at x=23.50 cm, the nature of the boundary layer is different due to the upstream bubble.
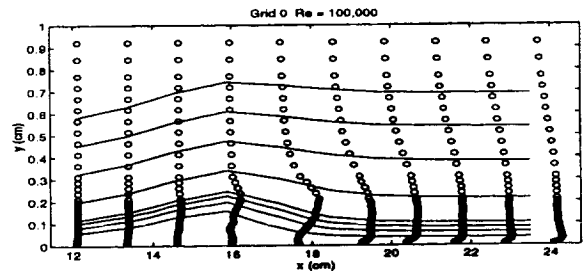

Figure 7. Distribution of u'_{rms}/U_{ref} Grid 0, Re=100,000 (U_{ref}=U_s at x=12.07 cm), $\Delta u'$= ± 0.00145
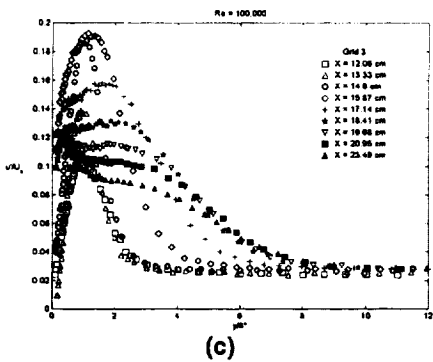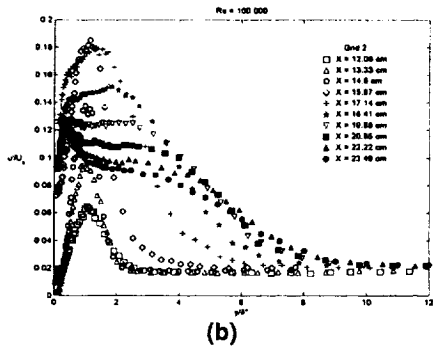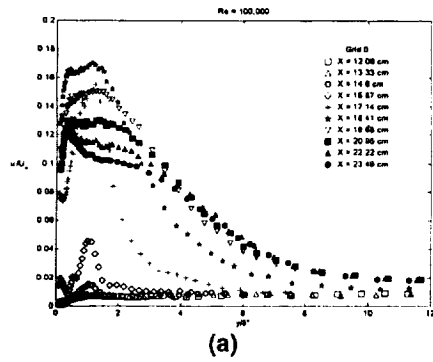
5

Figure 8a-c. RMS velocity profiles, Re =100,000
(a) Grid 0, (b) Grid 2 and (c) Grid 3, $\Delta u' = \pm 0.00145$

Classification of Separation Bubble

Gaster (1969) proposed a two parameter bubble criterion using a relationship between momentum Reynolds number at separation Re_{θ_s}, and pressure parameter $\bar{P} = (\theta_s^2/\nu)(\Delta U/\Delta x)$, based on his two sets of airfoil data and other researchers' experimental and calculated data. The pressure parameter, ΔU, is the rise in freestream velocity that would occur over the bubble length, Δx, in an unseparated inviscid flow. Gaster's two parameter-bursting criterions with pressure parameters measured in the present experiments are plotted in Fig. 9.

Three domains are defined in this figure. For $\bar{P} < -0.09$, the flow will not separate at any Reynolds numbers. To the right of the bursting boundary, a short bubble will be formed, and to the left, a long (bursting) bubble will develop. It is clear that the bubbles formed in the present experiment are all short ones. In the present experiment,

the inviscid pressure and ΔU are estimated from the Reynolds number of 250,000 at which the boundary layers are attached for the entire test section.
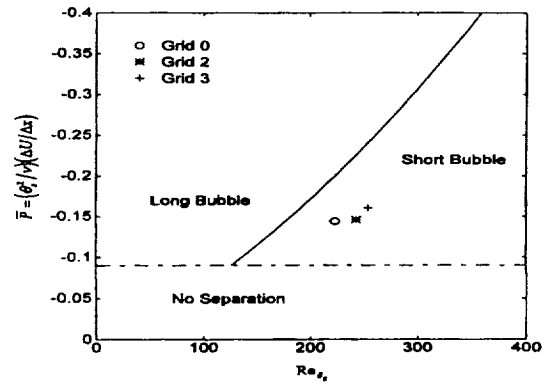

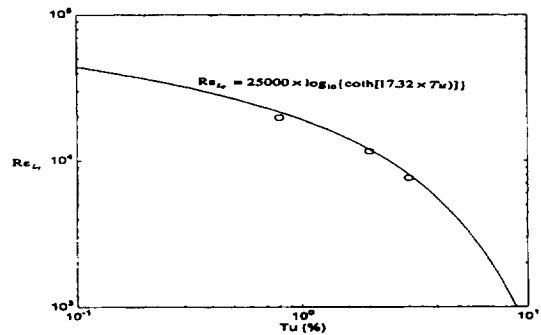**Figure 9. Gaster's two parameter bubble criteria**

Figure 10. Comparison of variation of transition length Reynolds number with freestream turbulence levels

Several empirical correlations have been developed accounting for the effects of freestream turbulence on the separation bubble length. Roberts (1980) related the transition length of the separation bubble to the turbulence scale factor, in which the turbulence scale is involved. The turbulence scale is a quantity not easily obtainable in experiments. Davis et al. (1985) modified the Roberts' correlation to replace the freestream turbulence factor with the local freestream turbulence level, i.e., $Re_{L_T} = 25000 \times \log_{10}\{\coth[17.32 \times Tu)]\}$. The variation of transition length Reynolds number at separation along with Roberts' modified correlation is presented in Fig. 10. The transition region determined from the intermittency profiles for each freestream turbulence level shows excellent agreement with this empirical correlation.

CONCLUSIONS

The parametric investigation of the flow field on a simulated LPT blade was performed at three levels of freestream turbulence for a Reynolds number of 100,000. The flow visualization data confirmed that the boundary layer was separated and formed a bubble. Based on a two-parameter bubble-bursting criterion proposed by Gaster (1969), the bubbles formed in these experiments were short, non-bursting

6

bubbles.

Flow visualization photographs revealed that the laminar portion of the bubble is steady, while the regions downstream from transition are unsteady. The transition process over the separated flow regions for a Reynolds number of 100,000 is similar to a laminar free shear layer through the formation of a large coherent eddy structure. However, the transition path for an attached boundary layer is through the formation of intermittent turbulent spots. These two distinct transition mechanisms were confirmed by a series of instantaneous hot-film signals. The pressure distribution shows a typical feature, namely a nearly constant pressure zone followed by a sharp pressure rise region. Intermittency profiles showed that shear flow transition initiated between x=14.60 and 15.87 cm for grid 0, at approximately x=14.60 cm for grid 2, and before x=14.60 cm for grid 3. Additionally, the intermittency profiles revealed that fully turbulent flow occurs approximately at x=18.41 - 19.68 cm for grid 0, at x=17.14 cm for grid 2, and between x=15.87 - 17.14 cm for grid 3. The transition onset location and length are inversely proportional to the freestream turbulence level. Additionally, the characteristics of transition deduced from the intermittency profiles and boundary layer spectra data show excellent agreement. The modified Roberts' transition length correlation predicts quite well the transition length of the bubble for each condition. It was also observed that bubble length and height decreased as freestream turbulence level increased. Additional experimental work is currently being conducted at lower Reynolds numbers and various freestream turbulence levels to identify the conditions at which the separation bubble may burst.

REFERENCES

Davis, R. L., Carter, J. E., and Reshotko, E., 1985, "Analysis of Transitional Separation Bubbles on Infinite Swept Wings," AIAA-85-1685.

Gardner, W. B., 1981, "Energy Efficient Engine Low Pressure Turbine Boundary Layer Program Technology Report," NASA CR-165338.

Gaster, M., 1969, "The Structure and Behavior of Laminar Separation Bubbles," A.R.C. R&M 3595.

Halstead, D. E., Wisler, D. C., Okiishi, T. H., Walker, G. J., Hodson, H. P., and Shin, H., 1995, "Boundary Layer Development in Axial Compressors and Turbines, Part 3 of 4: LP Turbines," ASME Paper 95-GT-463.

Klebanoff, P.S. 1955, "Characteristics of Turbulence in a Boundary Layer with Zero Pressure Gradient," NACA Rep. No. 1247.

McFarland, E. R., 1982, "Solution of Plane Cascade Flow Using Improved Surface Singularity Methods," Journal of Engineering for Power, Vol.104, pp. 668-674.

Morin, B. L., and Patrick, W. P., 1991, "Detailed Studies of a Large-Scale Laminar Separation Bubble on a Flat Plate: Volume 1 - Experimental Technique, Summarized Results, and Discussion," UTRC Rep. R91-956786-1.

Roberts, W. B., 1980, "Calculation of Laminar Separation Bubbles and Their Effect on Airfoil Performance", AIAA Journal, Vol. 18, No. 1, pp. 25-30.

Shyne, R. J. , 1998, "Experimental Study of Boundary Layer Behavior in a Simulated Low Pressure Turbine," Ph.D. Dissertation, University of Toledo, NASA TM-1998-208503.

Sohn, K. H. and Reshotko, E., 1991, "Experimental Study of Boundary Layer Transition with Elevated Freestream Turbulence on a Heated Flat Plate," NASA CR-187068.

Suder, K. L., O'Brien, J. E., and Reshotko, E., 1988, "Experimental Study of Bypass Transition in a Boundary Layer," NASA TM-100913.

Yavuzkurt, S., "A Guide to Uncertainty Analysis of Hot-Wire Data", Journal of Fluids Engineering, Vol. 106, June 1984, pp. 181-186.

Table 1. Longitudinal integral length scale (cm)

	Grid 0	Grid 2	Grid 3
Re = 100,000	0.53	1.57	3.04
Re = 250,000	0.84	1.88	3.40

Table 2. Separation bubble characteristics

	X_s (cm)	X_R (cm)	L_B (cm)	H_B (cm)
Grid 0	$\approx$13.34	$\approx$17.40	$\approx$4.06	$\approx$0.110
Grid 2	$\approx$13.34	$\approx$15.88	$\approx$2.54	$\approx$0.056
Grid 3	$\approx$13.34	$\approx$14.86	$\approx$1.52	$\approx$0.030

TECHNICAL ASSOCIATE EDITORS
(full addresses overleaf)

Fluid Application and Systems
MANORANJAN N. DHAUBHADEL (1999)
Case Coporation
630-887-2009

BRUNO SCHIAVELLO (1999)
Ingersoll–Dresser Pump Company
908-859-7610

Fluid Measurements
SANJOY BANERJEE (1999)
University of California, Santa Barbara
805-893-3456

Fluid Mechanics
PETER W. BEARMAN (2001)
Imperial College of Science,
Technology and Medicine
44-171-594-5055

PETER BRADSHAW (2000)
Stanford University
650-725-0704

PETER E. RAAD (2001)
Southern Methodist University
214-768-3043

DAVID R. WILLIAMS (2000)
Illinois Institute of Technology
312-567-3192

KHAIRUL B.M.Q. ZAMAN (2001)
NASA Lewis Research Center
216-433-5888

Computational Fluid Dynamics
GORDON ERLEBACHER (2000)
Florida State University
850-645-0308

URMILA GHIA (2001)
University of Cincinnati
513-556-4612

CHARLES L. MERKLE (2000)
University of Tennessee Space Institute
931-393-7426

Multiphase Flow
JOHN K. EATON (1999)
Stanford University
650-723-1971

JOSEPH KATZ (2001)
The Johns Hopkins University
410-516-5470

MARTIN SOMMERFELD (1999)
Martin-Luther-Universitat Halle-Wittenberg
49 3461-462879

FREDERIC K. WASDEN (2000)
Shell E&P Technology Company
281-544-7909

Editorial Office
MUHAMMAD R. HAJJ (2001)
Virginia Polytechnic Institute and State University
540-231-4190

August 30, 1999

Dr. Rickey J. Shyne
Senior Research Engineer
NASA Glenn Research Center
Lewis Field
Cleveland, OH 44135-3191

Re: Experimental Investigation of Boundary Layer Behavior in a
      Simulated Low Pressure Turbine (Log No. 5118-DRW)

Dear Dr. Shyne:

I have read your paper, as well as the reviews and comments of the associate
editor. I basically agree with the recommendations of Dr. Williams. I am,
therefore, pleased to inform you that your paper has been accepted for
publication in the *Journal of Fluids Engineering*. Your paper is scheduled
for the December issue.

There is now another option you should keep in mind. In case you do not
know, the *Journal of Fluids Engineering* is already on the Web
(http://www.asme.org). To access click on Publications choose Journals
and then select Fluids Engineering. All the printed papers are available in
exactly the same format but there is room for addenda. These could be
extra figures in black and white or color, lengthy derivations, computer
codes or digital data. If you want to add any such material to this paper, you
can still do so if you act immediately. You can send this material on a disk
to me to be reviewed and edited. If you have any questions you could
contact directly the Data Bank Webmaster, Dr. Norman Schaeffler at
nschaeff@vt.edu.

We need a set of original figures. Also the printer prefers double-spaced
single-column copies of your paper. In order to include your paper in the